Apr 1st, 8:00 AM

Systematic Atmospheric Refreaction Errors of Baseline Type Radio Tracking Systems and Methods for their Correction

G. D. Thayer

B. R. Bean

Follow this and additional works at: https://commons.erau.edu/space-congress-proceedings

SYSTEMATIC ATMOSPHERIC REFRACTION ERRORS OF BASELINE-TYPE RADIO TRACKING SYSTEMS AND METHODS FOR THEIR CORRECTION

by

G. D. Thayer and B. R. Bean

ABSTRACT

The theory of systematic atmospheric radio refraction errors affecting measurements of range and range differences (and associated time rate of change of these quantities) is developed. It is shown that the refraction errors, particularly in range difference measurements, can seriously affect the accuracy of baseline-type tracking systems. A method is derived by which the systematic portion of these errors can be removed by means of linear relationships involving the surface value of the radio refractive index; the correction process devised can be used in real time if desired. Several test cases are examined where horizontally-varying profiles of the refractive index variation with height are used to calculate the errors, and the correction process based on surface refractive index values is found to be useful under these more general conditions. Approximately 98 percent of the total range or range difference error can be removed using this correction procedure. The problem of baseline optimization for deep-space tracking is examined briefly, and it is shown that a baseline length of about 4,000 miles is optimal for targets more than about 6,000 miles from the earth, and for such a system residual atmospheric refraction errors would be only a few hundredths of a microradian, assuming the validity of ray optics and of the models of the atmosphere used in this paper.

SYSTEMATIC ATMOSPHERIC REFRACTION ERRORS OF BASELINE-TYPE RADIO TRACKING SYSTEMS AND METHODS FOR THEIR CORRECTION

by

G. D. Thayer and B. R. Bean
National Bureau of Standards
Boulder, Colorado

1. Introduction and Background

Errors in measurements of distance made with radio equipment are caused in part by the refractive nature of the atmosphere: the velocity of propagation of a radio wave is a function of the refractive index structure over the propagation path, and the path itself is distorted from a straight line by refraction of the radio wave front. For the purpose of this paper a radio range error will be defined as the difference between the true distance separating two points and the distance as measured by the transit time of radio signals between the two points. In this definition it is assumed that the measured value of range is computed as if the radio signals were transmitted in a straight line and using the in vacuo velocity of light.

Radio range errors are of considerable importance in determining the overall accuracy of modern radio tracking or guidance systems which utilize the principle of triangulation (in three-dimensional space) to locate target position. The basic geometry involved in such triangulations is shown in figure 1. Two antennas, A_1 and A_2, each measure a range, R_1 and R_2 respectively, to a common target point. These two ranges, plus the (surveyed) baseline, B form the three sides of a triangle $\overline{R_1 B R_2}$; the direction cosine to the target (from A_1 with respect to B) can be easily derived from the trigonometric law of cosines as:

$$\cos \beta = \frac{R_1^2 - R_2^2 + B^2}{2 R_1 B} . \tag{1}$$

Phase-locked systems measure the range R_1 and a range difference,

$$D R = R_1 - R_2 , \tag{2}$$

and in this case (1) may be rewritten in the form:

$$\cos \beta = \frac{D R}{B} + \frac{B^2 - D R^2}{2 R_1 B} . \tag{3}$$

142

The target position is determined by measuring another direction cosine with respect to a second baseline from A_1 to a third antenna A_3 (not shown).

The error due to refraction effects in the range difference measurement is simply the difference between the radio range errors of R_1 and R_2 in (2). Throughout the remainder of this paper the terms range error and range difference error will refer to atmospheric (not ionospheric) refraction errors which will be denoted by the operator Δ, while a range or range difference measurement containing a refraction error will be starred; thus from (2):

$$DR^* = R_1^* - R_2^* \ ,$$

$$DR + \Delta DR = R_1 + \Delta R_1 - (R_2 + \Delta R_2) \ ,$$

$$\Delta DR = \Delta R_1 - \Delta R_2 \ . \tag{4}$$

The error in the direction cosine due to the range errors ΔR_1 and ΔR_2 can be found by deriving the differential of the function $\cos \beta$ in (1), since the range errors are always very small compared to the ranges ($\Delta R/R < 0.0004$):

$$\Delta (\cos \beta) \doteq \frac{R_2}{R_1} \frac{\Delta DR}{B} - \frac{B^2 - DR^2}{2 R_1^2 B} \Delta R_1 \ . \tag{5}$$

Equation (5) is asymptotically exact as the ratio $\Delta R_1/R_1$ approaches zero; (5) also reveals that there is no fundamental difference between the behavior of the phase-locked system and the independent range-finder system in that the largest portion of the direction cosine error in either case is a function of the range difference error. This is especially true for the case when $R_1 \gg B$, since the term involving ΔR_1 in (5) may be ignored (note that $DR \leqq B$ must always be true).

Direction cosine information can be corrected for the refraction errors if the range errors, and in particular the range difference errors, can be corrected. The actual value of the radio range error occurring over a given propagation path is a function of the structure of the atmospheric radio refractive index, n, along and in the immediate vicinity of the path at the time that the range measurement is made. This refractive index structure is always to some extent an unknown quantity, but the most pronounced feature is always a quasi-exponential decrease of the refractivity, $N(n-1) \times 10^6$, with height above the surface.[1] It follows that radio range errors will show some systematic behavior depending, for example, on how much (if any) of the propagation path lies in the upper atmosphere where the N values are lower than near the surface.

In the sections that follow, the ray-geometrical equations for single path range errors are developed, and it is shown that systematic correction are possible based on the surface value of the refractivity, N_s. The systematic refraction errors of baseline triangulation systems, defined as those errors occurring in a horizontally homogeneous atmosphere, are derived, and it is shown how they may be corrected. The resulting correction technique is

applied to some test cases involving horizontal inhomogeneity of the refractive index, and the results are in good agreement with the systematic predictions. Brief evidence is introduced that the systematic correction technique is also statistically optimum for correction of the non-systematic, random errors occurring under actual conditions. The results are extended to the case of very large baselines for tracking deep-space targets, and it is found that baselines on the order of 6700 km (4150 miles) are optimal (in the sense of minimal residual refraction errors) for tracking targets at distances of 10,000 km (6,000 miles) or more; the resulting rms residual direction angle errors range from about 0.01 to 0.05 microradians, assuming the validity of ray optics and of the models of the atmosphere used in this paper.

2. Theory and Correction of Systematic Radio Range and Range Difference Errors

The theory of radio range errors is most easily developed within the framework of ray-geometrical optics[2] (Fresnel approximation). In this notation the apparent radio range between two points is expressed as a line integral along the ray path connecting the points:

$$R_e = \int_0^{R_g} n\{s\}\, ds, \tag{6}$$

where $n\{s\}$ is the refractive index as a function of position on the ray path, ds is the differential of ray path length, and R_g is the true length of the (curved) ray path between the points. Normally the origin of the ray path is taken to be the radio antenna and the upper terminal is the target position. Figure 2 shows ray tracing geometry. It is convenient to rewrite (6) as:

$$R_e = \int_0^{R_g} ds + 10^{-6} \int_0^{R_g} N\{s\}\, ds, \tag{7}$$

where N is the refractivity, $(n-1) \times 10^6$ in parts-per-million (ppm). The range error is now obtained by subtracting the true range, R_o, from the apparent range given by (7):

$$\Delta R = R_g - R_o + 10^{-6} \int_0^{R_g} N\{s\}\, ds. \tag{8}$$

The quantity $R_g - R_o$ in (8) can be called the geometric radio range error, ΔR_g, as it is caused only by the distortion of the ray path from a straight line, while the integral in (8) represents the error caused by the reduction in velocity of the wavefront in the refractive medium, and can be called the N-related range error, ΔR_N. Table I shows ray-traced values of both ΔR_g and ΔR_N for a typical N-profile ($N_s = 320$) and an extreme N-profile ($N_s = 400$). It can be seen that ΔR_N is the dominant quantity even at very small elevation angles.

144

Table I

Typical and Extreme Values of Range Errors for Targets
Beyond the Atmosphere

θ_o Milliradians	Typical $N_s \cong 320$			Extreme $N_s \cong 400$			Maximum %
	ΔR_g	ΔR_N	ΔR_e	ΔR_g	ΔR_N	ΔR_e	$\Delta R_g / \Delta R_e$
	Meters			Meters			
0	10	100	110	60	165	225	~27%
20	2.5	62.5	65	4.5	73	77.5	6%
50	0.7	38.1	38.8	1.0	43	44	2.3%
100	0.14	22.26	22.4	0.2	24.8	25	0.8%
200	0.02	11.9	11.9	0.03	13.0	13.0	0.23%
500	0.001	5.01	5.01	5.01	0.002	5.50	0.04%

A convenient quantity to study is the relative radio range error, defined as $\Delta R/R_o$, which is given in ppm by:

$$\frac{\Delta R}{R_o} \text{(ppm)} = \frac{1}{R_o} \int_0^{R_g} N\{s\}\ ds + \frac{\Delta R_g \times 10^6}{R_o}\ , \qquad (9)$$

or

$$\frac{\Delta R}{R_o} \text{(ppm)} \cong \frac{1}{R_g} \int_0^{R_g} N\{s\}\ ds + \frac{\Delta R_g \times 10^6}{R_o}\ , \qquad (10)$$

since R_g will not differ by more than about 10 ppm from R_o under non-ducting conditions. As can be seen from (10), the bulk of the radio range error is essentially the average of $N\{s\}$ taken over the ray path.

The refractivity, N, may be written as the sum of two variables: the "expected value", $\langle N \rangle$, which is essentially only a function of altitude, and a zero-mean random component N', whose statistical distribution may also be a function of altitude. Rewriting (10) with N defined in this manner, and the differential ds replaced by the equivalent $dh\ \csc\theta$ (where θ is the local ray elevation angle and dh is the differential of height):

$$\frac{\Delta R}{R_o} \text{(ppm)} \cong \frac{1}{R_g} \int_0^{R_g} \langle N\{h\} \rangle \csc\theta\ dh + \frac{1}{R_g} \int_0^{R_g} N'\{s\}\ ds + \frac{\Delta R_g \times 10^6}{R_o} \qquad (11)$$

The variable $\langle N\{h\} \rangle$ is identified with very long time averages of N measured at a particular height h, above the surface in the vicinity of the ray-path origin (since $\langle N\{h\} \rangle$ does vary to some extent with latitude, etc.). $N'\{s\}$ then represents the deviations of $N\{s\}$ from the expected values $\langle N\{h\} \rangle$ which are taken to be the same as $\langle N\{h\} \rangle$, where h corresponds to the height of the point s on the ray path. The $\langle N\{h\} \rangle$ profile thus constitutes a sort of standard atmosphere; it has been found that standard atmospheres which are a function of the observed surface N value, N_s, are good predictors of refraction effects.[1, 3] Thus the "expected value" of range error, or what might be called the "systematic" range error, may be defined as the long time average of (11) for all cases where the N_s value is the same:

$$\left\langle \frac{\Delta R}{R_o} \right\rangle \text{(ppm)} \cong \left\langle \frac{1}{R_g} \right\rangle \int_0^{R_g} \langle N\{h\} \rangle \langle \csc\theta \rangle\ dh + \left\langle \frac{\Delta R_g}{R_o} \right\rangle \times 10^6\ , \quad N_s = \text{const.} \ , \qquad (12)$$

the expected value of the second integral in (11) vanishing since the $N'\{s\}$ have zero mean (the rms or second moment would not vanish, and defines the limit of accuracy of predicting $\frac{\Delta R}{R_o}$ from $\left\langle \frac{\Delta R}{R_o} \right\rangle$).

146

Applying the second theorem of the mean for integrals to (12) one obtains:

$$<\frac{\Delta R}{R_o}> (ppm) \cong \frac{<\csc \theta_1>}{<R_g>} \int_0^{<R_g>} <N\{h\}> dh + <\frac{\Delta R_g}{R_o}> \times 10^6, \quad N_s = const \quad (13)$$

where $<\csc \theta_1>$ is $<\csc \theta>$ evaluated at some point on the (mean) ray path. It turns out that for initial angles, θ_o, larger than about 10°, the value $<\csc \theta_1>$ is essentially just $\csc \theta_o$ (i.e. $\csc \theta$ is nearly constant over the part of the ray path where $<N\{h\}>$ is much larger than zero). Thus the systematic range error is expected to be primarily a function of the integral of $<N\{h\}>$ with respect to height. It is not surprising that this integral is a function of the $<N_s>$ value, since that value defines the lower limit of the integral.

Figures 3 and 4 show ray-traced range errors for the CRPL Standard Radio Refractive Index Profile Sample[*, 3] Figure 3 for $\theta = \pi/2$ radians (90°) shows the behavior of the integral of $N\{h\}$ with respect to height for each profile, while figure 4 shows the total range error at $\theta_o = 50$ mr (about 3°), both as a function of N_s. The regression lines show the best (linear) estimate of $<\Delta R>$ as a least squares fit; the scatter of the individual points shows the effect of the integral of $N'\{s\}$ ds as in (11), plus whatever small error is incurred by predicting ΔR_g as a linear function of N_s for the $\theta_o = 50$ mr case. The reader should especially note the strong similarity of the distribution of points in figures 3 and 4; this indicates that the behavior of range errors at relatively small elevation angles is still primarily a function of the average of $N\{h\}$ over the target height interval, and that errors in predicting ΔR_g are of negligible effect at least for $\theta_o \gtrsim 50$ mr.

It will be noted that it was necessary to introduce a correction for station elevation above mean sea level because of the wide range of elevations encountered in the standard sample (8 m to 1908 m); for a single station this term would of course drop out, so it may be regarded as an adjustment to the constant term of the linear equation in N_s. The resulting correction procedure is a system of linear equation coefficients, such that:

$$<\Delta R> = a\{h_t, R, h_s\} + b\{h_t, R\} N_s, \quad (14)$$

where h_t is target height, R is apparent range, and h_s is surface elevation above mean sea level.

The systematic refraction error of the baseline tracking system is given by (5) using expected values for ΔR, and ΔDR, the latter being defined as:

$$<\Delta DR> = <\Delta R_1> - <\Delta R_2>. \quad (15)$$

The systematic errors are corrected for by use of the system of linear equations used to predict $<\Delta R>$ as a function of observed N_s values. The residual error involved in correcting actual (real time) values of $\Delta(\cos \beta)$ by removing the

---

* See Appendix

systematic component $<\Delta(\cos\beta)>$ are of interest since they define the rms residual error in $\cos\beta^*$ after corrections have been made for observed N_s values. The residual variance of $\Delta(\cos\beta)$ produced by residual variances in ΔDR and ΔR_1 may be found by taking the statistical second moment of (5), leading to:

$$S^2\{\Delta(\cos\beta)\} \doteq \left(\frac{R_2}{R_1}\right)^2 \frac{S^2_{R_1} + S^2_{R_2} - 2r_B S_{R_1} S_{R_2}}{B^2} + \left(\frac{B^2 - DR^2}{2R_1^2 B}\right) \times$$

$$\left[\frac{B^2 - DR^2}{2R_1^2 B} - \frac{2R_2}{R_1 B}\right] S^2_{R_1} + \frac{2R_2}{R_1 B} r_B S_{R_1} S_{R_2} \left(\frac{B^2 - DR^2}{2R_1^2 B}\right), \quad (16)$$

where $S^2_{R_1}$, $S^2_{R_2}$ are the residual variances in predicting ΔR with $<\Delta R_1>$ and ΔR_2 with $<\Delta R_2>$, and r_B is the correlation coefficient between $\Delta R_1 - <\Delta R_1>$ and $\Delta R_2 - <\Delta R_2>$ for the particular baseline under consideration; the value of r_B is expected to be a decreasing function of increasing baseline length.

If it is assumed that the target is located at a range (R_1) very much larger than the baseline, B, then the last two terms of (16) may be neglected (and the last term of (5) as well), and R_2/R_1 approaches unity; in this case:

$$S^2\{\Delta(\cos\beta)\} \doteq \frac{S^2_{R_1} + S^2_{R_2} - 2r_B S_{R_1} S_{R_2}}{B^2}, \quad R_1 \gg B. \quad (17)$$

It is found both theoretically and experimentally that the residual variance of radio range errors after N_s correction tend to be proportional to the square of the expected value of the range error, $<\Delta R_1>$, so (17) may be rewritten:[3,4]

$$S^2\{\Delta(\cos\beta)\} \cong \frac{S^2_{R_1}}{B^2}\left[1 + \left(\frac{<\Delta R_2>}{<\Delta R_1>}\right)^2 - 2r_B\left(\frac{<\Delta R_2>}{<\Delta R_1>}\right)\right], \quad R_1 \gg B. \quad (18)$$

The systematic residual refraction error in the direction cosine can now be **defined** by the variance as given by (18), with the further assumption of horizontal homogeneity of the refractive index structure, which simply assumes $r_B = 1$ for all baselines:

$$S^2_H\{\Delta(\cos\beta)\} \cong \frac{S^2_{R_1}}{B^2}\left[1 + \left(\frac{<\Delta R_2>}{<\Delta R_1>}\right)^2 - 2\left(\frac{<\Delta R_2>}{<\Delta R_1>}\right)\right], \quad R_1 \gg B, \quad (19)$$

148

where S_H^2 indicates the residual variance under the horizontal homogeneity assumption.

Numerical calculations have been performed to determine the systematic direction angle error of baseline systems under the stated conditions, using a modification of (5):

$$\Delta \beta \cong \frac{<\Delta R_1> - <\Delta R_2>}{B} \ \csc \beta \ , \qquad R_1 \gg B , \qquad (20)$$

the results are shown in figure 5, together with total ray refraction which affects ordinary radar.[5] The residual standard deviations of the systematic errors were calculated from

$$S_H\{\Delta\beta\} \cong \sqrt{S_H^2\{\Delta(\cos\beta)\} \ \csc^2\beta} \ , \qquad R_1 \gg B , \ r_B \equiv 1 , \qquad (21)$$

where $S_H^2\{\Delta(\cos\beta)\}$ is given by (19). These errors are shown in figure 6.

Note that (19) yields a null result for cases when $<\Delta R_1> = <\Delta R_2>$, which occurs whenever the target is located equidistant from the two ends of the base line. In real systems there will be some residual error in all cases; this is because $r_B < 1$ for any real baseline. Thus it is logical to call the error contribution in (16) or (17) due to $r_B < 1$ the stochastic or random error of the system. Such errors can be derived theoretically, and are calculated in a forthcoming paper.[4] The results are presented here for comparison with figure 6, the total error having been calculated as:

$$S^2 \ \Delta(\cos\beta)\} \cong S_H^2\{\Delta(\cos\beta)\} + \frac{S_{R_1}^2}{B^2} \ \left(\frac{<\Delta R_2>}{<\Delta R_1>}\right) 2 \left[1 - r_B\right],$$

and

$$S\{\Delta\beta\} \cong \sqrt{S^2\{\Delta(\cos\beta)\} \ \csc^2\beta} \ , \qquad R_1 \gg B . \qquad (22)$$

These total residual errors are shown in figure 7. Also shown in figure 7 are total residual error estimates for tracking radar, $(R_B \approx 1)$ where the random component (angular scintillation) has been found in two different ways: by extrapolation of the baseline random component to zero baseline (the movable radar antenna sees essentially the direction cosine error since its direction angle is always 90°), and by empirical curve-fitting to the Collins Radio Company data.[3]

The accuracy of these systematic corrections when applied to actual (experimental) range error data has been examine in an earlier paper, with satisfacotry results.[3] For the shorter baselines, however, the random uncorrelated component of residual error is the dominant term in (22), and the errors shown

---

*Shared baseline operation is discussed following (25).

in figure 7 are considerably larger than those shown in figure 6 for the base lines shorter than 300 km. It should be pointed out, however, that there is still a noticeable reduction (attributable to the N_s correction technique) in the overall rms errors for all baselines larger than about 3 km. In cases where the target is located relatively close to the baseline (i.e.: R_1 or $R_2 \approx B$), the N_s correction technique would be valuable even for very short baselines.

3. Examination of Residual Direction Angle Errors for an Atmosphere Containing Horizontal Inhomogeneities

As a part of a study on the effects of atmospheric refraction on the precision of radio baseline triangulation systems, sometimes called "radio interferometers"[6], an analysis was made of the errors in range differences taken over rather long baselines in a horizontally inhomogeneous atmosphere. Four profiles were obtained, each from a number of radiosonde ascents made at approximately the same time at stations located roughly in a straight line covering a distance of about 750 miles. Figure 8 shows the two-dimensional profiles obtained in this way. Figure 8 is plotted in terms of A-units:[7]

$$A = N\{h\} + N_s \left[1 - \exp\left\{\frac{h}{7}\right\} \right] \tag{23}$$

a convenient quantity which represents approximately potential surface refractivity, and thus emphasizes horizontal N-changes while masking the normal quasi-exponential vertical N-gradient. It is felt that these represent more the extremes of horizontal inhomogeneity than typical values, since the times for which the profiles for each path were assembled were chosen by a meteorologist using daily synoptic weather maps, attempting to find situations where the contrasts in air mass characteristics along the path were maximized.

Four hypothetical baselines were drawn on each of the four profiles, with baseline lengths of 3, 30, 300 and 1000 km, all with one common antenna location, and the second at the various distances specified. A hypothetical target was then assumed to be placed at an altitude of 70 km, and refraction analyses were performed with the target making a true elevation angle at the common antenna of 20, 50, 100, 200, and 500 milliradians (approximately $1°$, $3°$, $6°$, $11\frac{1}{2}°$, and $29°$). The three kilometer baseline could not actually be analyzed as such because of limitations in the resolution which could be obtained from the graphical profiles, hence this baseline was analyzed from the common antenna ray path data as a horizontally homogeneous control case. Thus this horizontal inhomogeneity study applies only to the 30, 300, and 1000 km baselines.

Radio range errors were analyzed for each case by means of iterative ray-tracing techniques, and the range differences and resulting direction angle errors were calculated on a digital computer. In this connection, three important facts should be noted: 1) the direction angles were computed for the common antenna; 2) a standard refractivity atmosphere was assumed to exist at altitudes larger

than those covered on the charts, as it was noted that horizontal changes did not seem to be significant above that point; 3) the target was assumed to be in a direction such that it would be located between the antennas of the longest baselines. The last was done to avoid putting the long baselines at too much of a disadvantage with respect to the short baselines, as the 70 km target height was already a disadvantage: at the 500 mr angle the secondary antenna of the 1000 km baseline has a look angle of only about 20 mr.

The results of these calculations are summarized in Table II. The rms direction angle errors for all four propagation paths are listed for each baseline and elevation angle, as well as the residual errors after correcting for the expected range errors with available N_s data. The residual errors are also shown as a percentage of the mean uncorrected direction angles, $\overline{\Delta\beta}$, listed in the table.

The N_s corrections were made using two methods, listed as I and II in the table. Method I consisted of making a purely systematic range difference correction by using the N_s value from the common antenna location to correct both range errors. Method II consisted of using separate N_s values at each end of the baseline* to correct the range errors independently: method II thus makes an attempt to correct for horizontal inhomogeneities between the two ray paths.

For comparison, theoretical values of residual direction angle error have been calculated using (16) and the second equation in (22). In these calculated from the tabulated values of $\overline{\Delta R_1}$ and $\overline{\Delta R_2}$, taking advantage of the empirically observed fact that for a target height of 70 km the rms residual error in predicting ΔR from N_s is 1.7% of the mean values of ΔR (for the CRPL Standard Sample). [3] The percentage errors were then calculated using the tabulated values of $\overline{\Delta\beta}$. These theoretical values were calculated for the extreme cases of $r_B = 0$ and $r_B = 1$ in (16); in the case of $r_B = 1$, or a perfectly homogeneous atmosphere, the residual percentage direction angle errors are all 1.7%, the same as for the individual range errors.

It is obvious from inspection that the residual errors for the shorter baselines are closer to the theoretical values for $r_B = 1$, and for the longer baselines closer to $r_B = 0$. The case of B = 1000 km, $\theta_o = 100$ mr, is close to the case mentioned previously where $\langle \Delta R_1 \rangle = \langle \Delta R_2 \rangle$, and is apparent that the N_s correction is not of great utility in this instance. Also of interest is that method I seems superior to method II for B = 30 km, and about even for B = 300 km. This implies that a single average N_s reading will be most useful in correcting errors for baselines of 30 km or less, using these methods.

It is possible to derive from the data going into this study the approximate observed values of r_B as a function of baseline length. Unfortunately, from such a limited sample the variations of observed values of r_B are quite large for each baseline, and not much confidence can be attached to even the mean for a given baseline. However, keeping this in mind, the value of r_B for the 30 km baseline seems to be in the neighborhood of 0.97 - 0.98 (which is probably too high), for the 300 km baseline about 0.4 to 0.6, and for the 1000 km baseline and about 0 to 0.4. These compare with theoretical values of 0.7, 0.3, and 0.13, respectively.[4]

---

*As shown in figure 8

Table II
RMS Range Difference Errors with Horizontally Inhomogeneous
Refractivity Structure; for h_T = 70 km.

Baseline (km)	Elev. Angle (mr)	$\overline{\Delta R}_1$ (m)	$\overline{\Delta R}_2$ (m)	$\overline{\Delta\beta}$ (μrad)	S(Δβ) method I (μrad)	method II (μrad)	% S(Δβ) I	II	Expected % S(Δβ) $r_B \equiv 0$	$r_B \equiv 1$
3	20	56.1	55.6	12,655	179	--	0.5%	--	240%	1.7%
	50	36.2	35.9	2,084	38.5	--	3.3%	--	280%	''
	100	21.7	21.5	634.5	8.40	--	2.2%	--	270%	''
	200	11.7	11.5	213.9	3.83	--	1.7%	--	220%	''
	500	4.95	4.86	63.80	0.832	--	2.4%	--	130%	''
30	20	56.1	51.3	8,624	134	408	1.6%	4.7%	27%	1.7%
	50	36.2	33.2	1,823	91.2	116	5.0%	6.4%	28%	''
	100	21.7	19.8	561.4	20.0	29.9	3.6%	5.3%	27%	
	200	11.7	10.4	183.8	6.29	8.26	3.4%	4.5%	16%	
	500	4.95	4.06	50.75	1.34	1.42	2.6%	2.8%	12%	
300	20	56.1	23.7	1,457	25.6	44.7	1.8%	3.1%	3.2%	1.7%
	50	36.2	15.1	473.2	30.1	29.4	6.4%	6.2%	3.2%	
	100	21.7	7.6	130.2	1.42	3.14	1.1%	2.4%	2.8%	
	200	11.7	2.4	32.1	0.462	0.634	1.4%	2.0%	2.2%	
	500	4.95	6.69	16.31	1.38	1.17	8.5%	7.2%	8.1%	
1000	20	56.1	6.8	489.6	5.91	8.15	1.2%	1.7%	1.9%	1.7%
	50	36.2	12.7	241.8	2.77	5.32	1.2%	2.2%	2.8%	
	100	21.7	22.2	8.86	8.74	4.52	98.6%	51.0%	91.5%	
	200	11.7	38.8	317.5	20.8	7.65	6.6%	2.4%	2.5%	
	500	4.95	66.9	803.3	48.0	19.1	6.0%	2.4%	1.8%	

The most important conclusion derived from this particular study is that for small baselines (B > 30 km, or perhaps more) it is important to use a single value of N_s to predict the range errors for all antennas in the system, regardless of the number of instruments available for measuring N_s. In cases where a number of accurate instruments are available, the best procedure would seem to be to use the mean of all readings at any given time. For very long baselines, such as are advocated in Section 4 of this paper, it is important to correct the range errors for each antenna independently since for such separations r_B approaches zero. The reader can no doubt draw many more interesting conclusions from a careful examination of the data in Table II, as regards such things as the relative advantages of varying baselines under different target position configurations, etc.

4. Optimum Baseline Systems for Deep Space Tracking Applications

If a tracking system were to be built with two of the antennas located at opposite points on the earth's surface, i.e., a surface baseline of about 20,000 km, the system would only be able to "see" targets at extremely large ranges located very close to a plane perpendicularly bisecting the baseline, which would be a diameter of the earth. Such a system obviously would not be practical, but even more important, the residual tracking errors of such a system would be larger than for systems of somewhat smaller baselines because both ray paths would always be near zero initial elevation angles, and hence would traverse a portion of the earth's atmosphere effectively some 50 to 70 times "thicker" than that penetrated by a ray at near-vertical incidence. The question then arises as to what might constitute an optimum baseline length in terms of minimum residual direction angle error as a function of target range and elevation angle.

A theoretical study has been made of residual tracking errors for a large number of target positions and baseline lengths using a digital computer. In order to obtain results which would be as unbiased as possible, the target positions were restricted to heights beyond the earth's refractive atmosphere, the the calculations were made using geocentric target angle and true target height as target-to-baseline geometric parameters, as shown in figure 9. As can be seen the geocentric target angle is essentially the zenith angle referred to a point at the center of the baseline, but measured at the center of the earth. A value of $a_T = 0$ usually for any baseline at any given target height. The residual angle error for each case was determined as follows:

1. From the true geometry involved the true elevation angle (with respect to the earth's surface) was calculated for each antenna. The target is assumed to lie in a plane containing the baseline and the center of the earth.

2. The residual single-path range error for each antenna ray-path was then calculated using an empirical relationship

$$S_R = \frac{\pm 4.0 \times 10^{-5} \, (km)}{\sin \theta + \dfrac{2.94 \times 10^{-2}}{1 + 14\theta + 43\theta^2}} \tag{24}$$

where θ is the true elevation angle at the antenna in radians. This equation is quite accurate (error less than 1%) in giving the residual range error as determined by linear regression of ΔR versus N_s for the CRPL Standard Radio Refractive Index Profile Sample[3]. Note that the residual error at vertical incidence is given as ± 4.0 cm by (24).

3. The residual direction angle error was then calculated by solving (16) and (22) using (24) for the values of S_{R_1} and S_{R_2}, and using a theoretical form for r_B[4]. The function r_B is approximately zero for B > 2500 km.

Figure 10 shows some of the results of this study for target heights of 10^7 km to infinity. The curve marked "locus of critical points" represents the residual error for each baseline at the limiting geocentric target angle beyond which the target drops below the horizon for one of the antennas (the curve for a short baseline could, of course, cross this region if plotted). For $\alpha_T = 0$ the 10,000 km baseline is seen to be optimal, whereas for increasing values of α_T successively shorter baselines become optimal. It is obvious that baselines much longer than 10^4 km will never be optimal, since at lesser target ranges the shorter baseline is at even more of an advantage. In particular the impractical earth's-diameter system mentioned previously appears as a single point (labeled 20,000 km), and has a value of σ_ϵ (S $\{\Delta\beta\}$ in (22)) over 10 times as large as the more optimal baselines. It should be noted that the curve marked 6680 km is nearly optimal (within $\pm 14\%$ of optimum σ_ϵ) over a rather large range of α_T, from zero to nearly $\pm 50°$; the significance of this particular baseline length will be explained shortly.

Results for a true target height of 10,000 km are shown in figure 11. The limiting baseline is now seen to be about 15,000 km. The 6680 km baseline is seen to be optimal for this case up to geocentric target angles of about $\pm 30°$. The general level of the curves in the vicinity of $\alpha_T = 0$ is not much higher than for the case of near-infinite target range, but the shape of the curves is much "tighter" with respect to α_T; this is because of the "foreshortening" effect of the relatively close target position (close with respect to the baselines involved).

The results of this study can also be presented as a function of baseline with constant h_T or α_T, and the other as a curve parameter. Such a plot is shown in figure 12 for a constant geocentric target angle of $\pm 23°$. The locus of critical points represents the limiting value of baseline for each target height at $\alpha_T = 23°$, and the cross-hatched zone now represents a truly "forbidden" region. The 6680 km baseline (dashed vertical line) is now seen to be optimal or nearly so for target heights ranging from about 10,000 km to infinity. The angle of $23°$ is chosen since it is nearly equal to the earth's equatorial inclination ($23°27'$).

154

A deep-space tracking system would presumably be used for tracking/guidance of such things as lunar or interplanetary probes, (e.g., Mariner, Pioneer, etc.). This implies that the target of such systems would be generally located close to the plane of the ecliptic, which varies in declination (angle referred to earth's equatorial plane) by $\pm 23°27'$. The moon and all but one of the planets are restricted to declinations of about $\pm 30°$ or less, the lone exception being Pluto with $\pm 40°$ limits [cf. American Ephemeris & Nautical Almanac, various years]. Hence it appears that the logical location for a deep space tracking system with continuous tracking capabilities for deep space probes would be a series of east-west baselines located along or near the equator, with north-south baselines straddling them. The north-south baselines would then be required to track normally within a geocentric target angle of only $\pm 30°$. The required number of east-west baselines ranges from a minimum of two for the limiting case of zero baseline, each working at $a_T = \pm 90°$, to infinity for the other limiting case of 20,000 km baseline where each works only at $a_T = 0$. The required number is given by the formula

$$ j = \frac{2}{1 - \dfrac{B}{\pi r_o}} \tag{25} $$

where B is the baseline measured along the earth's surface and r_o is the radius of the earth; any fraction must be rounded off to the next larger whole number. Obviously the smallest practical value of j is three, for which the value of B/r may range up to $\pi/3$ or $60°$. At this point an interesting thing happens: one in effect has six different baselines; each of the six antennas of the original three east-west baselines being shared with one of the intervening baselines. This effect is shown in figure 13. Such a system can logically be called a "shared baseline", and will be so referred to in the remainder of this paper. The particular system illustrated in figure 13 is called "optimum shared baseline" because of the generally small tracking errors over the necessary range of target positions, as has already been pointed out, and because it requires only the practical minimum in equipment. The surface baseline of such a system is about 6680 km or 4150 miles. A shared baseline configuration with eight baselines and eight east-west antennas can be used with the resulting 5000 km baselines used for the smaller target ranges, and double baselines of 10,000 km used for large target ranges, but the residual error advantages over the six-baseline system would be very slight and probably not worth the extra cost involved.

The optimum shared baseline system must track equatorially only to geocentric target angles of $\pm 30°$ before an adjacent baseline picks up the target, and has already been pointed out the north-south baselines will probably not be required to track at over $\pm 30°$. The effect on either baseline of tracking a target off $30°$ both in declination (north-south geocentric angle) and in east-west geocentric angle is to increase the effective geocentric angle to about $\pm 35°$. This allows continuous tracking with a 6680 km baseline from a target height of about 10,000 km, (6000 miles), since the limiting angle for this case is about $\pm 38°$ (see figure 11).

155

To illustrate the overall tracking capabilities of the optimum shared base-line configuration, figure 14 has been prepared showing total target position error for several different target ranges (or heights) as the target passes over three of the east-west baselines at two declination angles. The total position error was calculated as the root-square-sum of the residual range error and the north-south and east-west position error (calculated as direction angle error times range):

$$\sigma \{P\} = \sqrt{\sigma_r^2 \{R\} + R^2 [\sigma_\epsilon^2 (n\text{-}s) + \sigma_\epsilon^2 (e\text{-}w)]}$$

The switching effect from one baseline to the next is clearly shown, especially for the R = 10,000 km case. The shared baseline effect is also illustrated in figure 7.

An example of a system of this type in use at the present time is the NASA Deep Space Instrumentation Facility (DSIF), which consists of three range and range rate stations located about 8000 miles apart near Goldstone, California, Johannesburg, South Africa, and Woomera, Australia. These independent trackers are capable of providing elevation and azimuth information with a precision on the order of 300 microradians, however when tracking a deep space probe, such as Mariner II, which follows a smooth orbit, advantage can be taken of redundancy techniques to utilize the four shared baselines inherent in the system. In this manner the trajectory of Mariner II was corrected to within a 10 mile uncertainty at closest encounter with Venus, at a range (from earth) of about 36 million miles, a residual error of only 0.28 microradians.[8] Figure 14 shows that under these conditions the theoretical minimum refraction error of the optimum shared base-line system would yield a position error of only about ± ½ mile, however the DSIF system accuracy was limited by range resolution and survey errors rather than refraction effects.

5. Conclusions and Discussion of Results

In summary, it has been shown that:

1.) It is possible to correct systematic range and range difference errors with a system of linear equations based on the use of surface refractive index observations.

2.) Under conditions of marked horizontal inhomogeneity of the refractive index structure the systematic corrections are still very useful, with the residual range errors increasing only about 30% over those for horizontally homogeneous conditions.

3.) For baselines of less than about 30 km (20 miles), all system range errors should be corrected using a single, averaged, N_s reading (theoretical considerations based on turbulence theory indicates that N_s readings should be averaged over a period on the order of 1½ to 2 hours for best results--see Reference 4).

4.) The optimum baseline lengths for deep space tracking are on the order of 4000 miles; potential tracking accuracies are a few parts in 100 million of target range.

The construction of baseline systems on the order of thousands of miles of separation poses a number of technical problems, in particular synchronization problems for cw systems which are presently causing difficulties over much shorter distances.[9] The solution would seem to lie in the direction of a number of independent range-only trackers.[10] There is also the problem of geological stability of the baselines: a shift of only five inches in 4,000 miles of the earth's crust would cause errors comparable to the residual refraction errors of such systems. However, it is possible that the use of artificial satellites for both baseline-calibration and synchronization between trackers could solve most of the problems associated with such large baselines. As an example of this technique, during the flight of Mariner II Jet Propulsion Laboratory Personnel, utilizing redundancy techniques, were able to use DSIF tracking data to reduce survey uncertainties for the three stations from 100 yards to 20 yards.[8]

6. Acknowledgements

References

1. Bean, B. R., and G. D. Thayer (May 1959). On models of the atmospheric radio refractive index, Proc. I.R.E. 47, No. 5, 740.

2. Born, M., and E. Wolf (1959). Principles of Optics, Pergamon Press, New York, N.Y.

3. Bean, B. R., and G. D. Thayer (May-June, 1963). Comparison of observed atmospheric radio refraction effects with values predicted through the use of surface weather observations, J. Res. NBS 67 D, (Radio Prop.) No. 3, 273-285.

4. Thayer, G. D., and B. R. Bean (1964). The effects of atmospheric refraction on the precision of radio range and range difference measurements, to be published in late 1964.

5. Bean, B. R., B. A. Cahoon, and G. D. Thayer (March 16, 1960). Tables for the statistical prediction of radio ray bending and elevation angle error using surface values of the refractive index, NBS Tech. Note No. 44, available from Office of Technical Services, Washington 25, D. C. price $.50.

6. Simmons, G. J. (1957) A theoretical study of errors in radio interferometer type measurements attributed to inhomogeneities of the medium, I.R.E. Trans. on Telemetry and Remote Control, TRC-3, 2-6.

7. Bean, B. R., L. P. Riggs, and J. D. Horn (1959). Synoptic study of the vertical distribution of the radio refractive index. J. Res. NBS 63 D, (Radio Prop.) No. 2, 249-254.

8. Jet Propulsion Laboratory staff (1963). Mariner: Mission to Venus, McGraw-Hill, New York.

9. Janes, H. B. (1963). Correlation of the phase of microwave signals on the same line-of-sight path at different frequencies, letter to the editor I.R.E. Trans. on Antennas and Propagation, Ap-11, No. 6.

10. Rutledge, C. K., R. A. Bowers, J. L. Culver, J. X. Mulvey, and G. H. Nowak (1961). Precise long range radar distance measuring techniques, Convair Report No. AE61-0061, 1 Feb. 1961.

The CRPL Standard Radio Refractive Index Profile Sample

The CRPL Standard Sample consists of 77 refractive index profiles obtained from radiosonde data for 13 U. S. Weather Bureau stations. The 13 stations were chosen to represent a cross-section of the climatic types found in the U.S.A. and vicinity, and range from semi-tropical (Miami, Fla.) to sub-arctic (Fairbanks, Alaska); the stations range in elevation from near sea level to over 6,000 feet (Ely, Nev.). Six profiles were chosen from individual radiosonde flights for each station, each of the six representing a particular type of profile: 26 of the profiles represent rather average conditions, while the other 51 each contain one or more abnormalities.(i.e.: surface duct, super-refractive ground layer, elevated duct, or a combination of these). This sample has been found to provide reliable estimates of refraction effects (as a function of N_s), as well as the variations and residual errors (after N_s correction) of these effects, when compared to actual data (see reference 3).
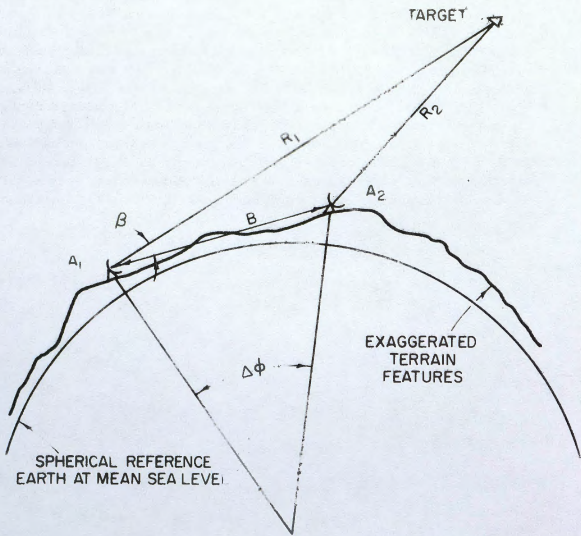
FIG I BASELINE TRACKING SYSTEM GEOMETRY
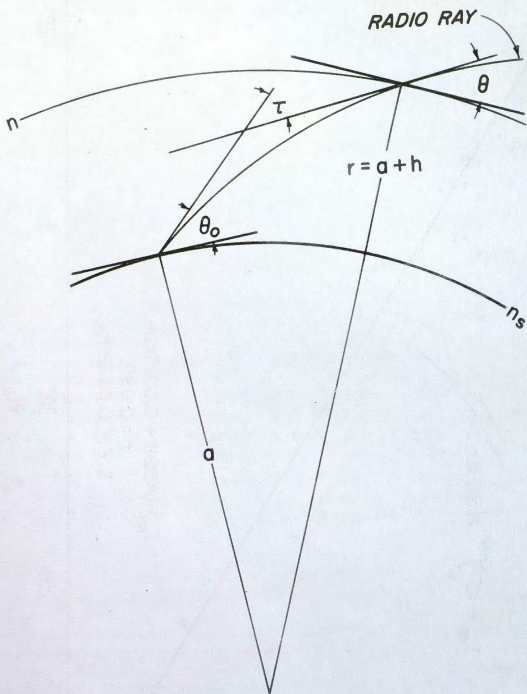
Figure 2. Geometry of radio ray refraction
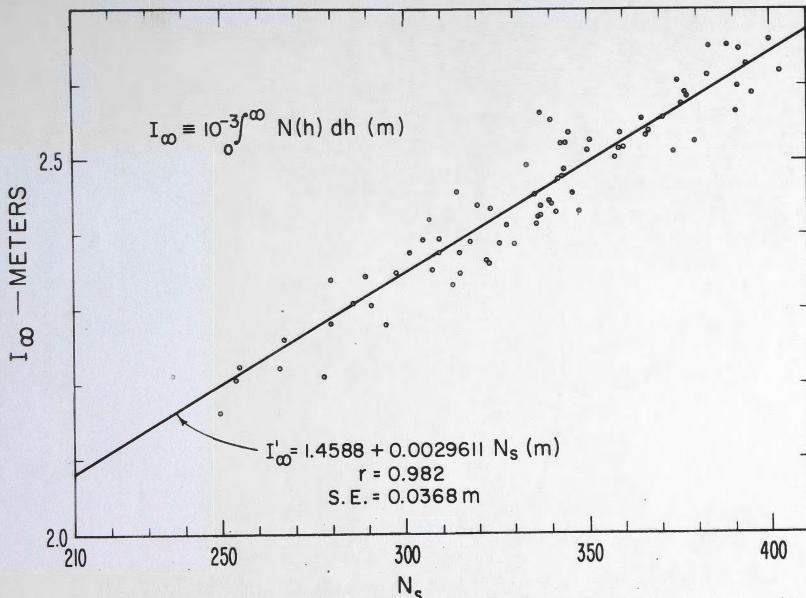
Figure 3. Integrated refractive index profiles for the CRPL Standard Sample. The integral of $N(h)$ with respect to height is taken from the surface to 70 km, above which point $N(h) \equiv 0$. The line represents the least squares regression of $I'(\infty)$ on N_s, where $I'(\infty)$ is the value of the integral as adjusted for the dependence on station (surface) elevation above mean sea level
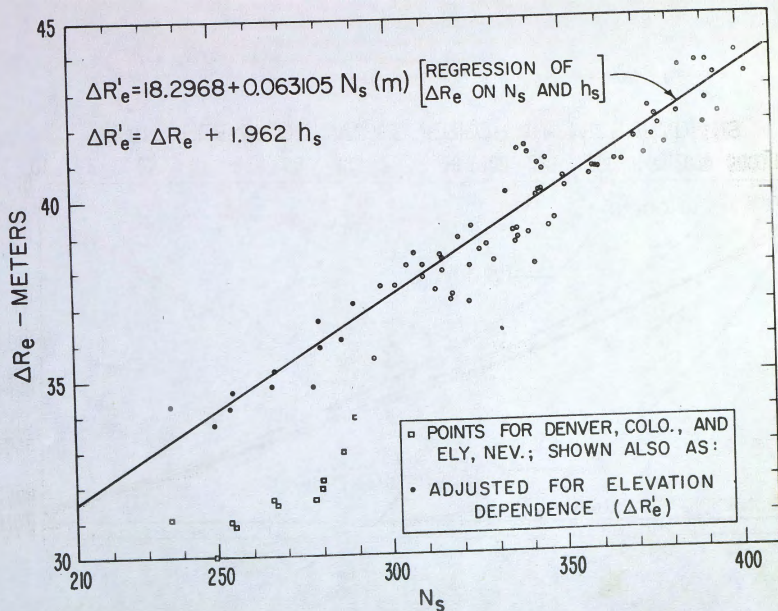
Figure 4. Total range error at $\theta_o = 50$ mr, $h_t = 70$ km, for the CRPL Standard Sample. The line indicates the least squares regression of $\Delta R'_e$ on N_s where $\Delta R'_e$ is the total range error adjusted for the dependence on station elevation.

$\Delta R'_e = 18.2968 + 0.063105 \, N_s$ (m) $\begin{bmatrix} \text{REGRESSION OF} \\ \Delta R_e \text{ ON } N_s \text{ AND } h_s \end{bmatrix}$

$\Delta R'_e = \Delta R_e + 1.962 \, h_s$

□ POINTS FOR DENVER, COLO., AND ELY, NEV.; SHOWN ALSO AS:

● ADJUSTED FOR ELEVATION DEPENDENCE $(\Delta R'_e)$

163
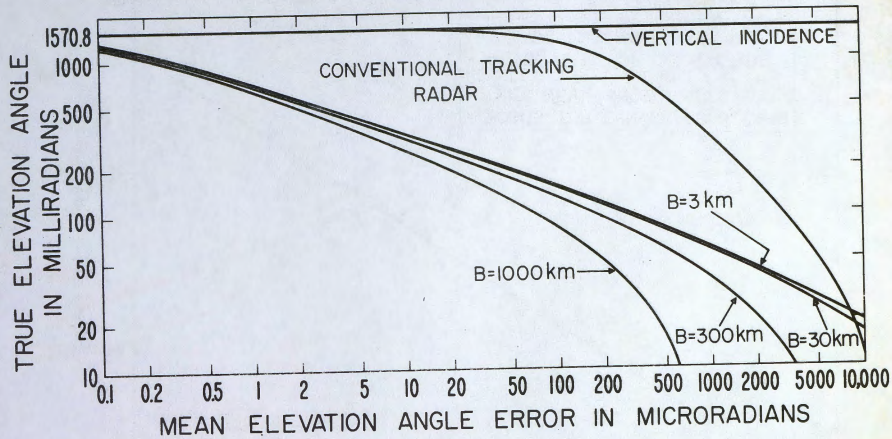
Figure 5. Average systematic refraction errors of baseline tracking systems for a target at infinite range (or R > 100 B).
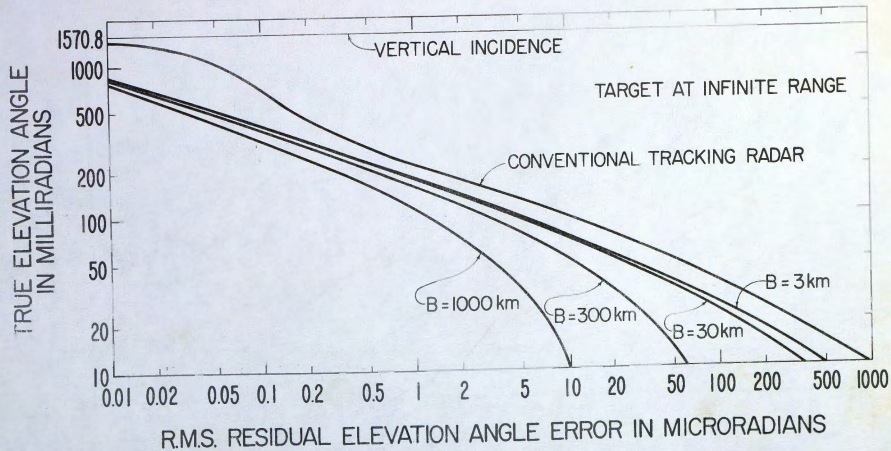
Figure 6. Residual rms systematic refraction errors of baseline tracking systems, target at infinite range.
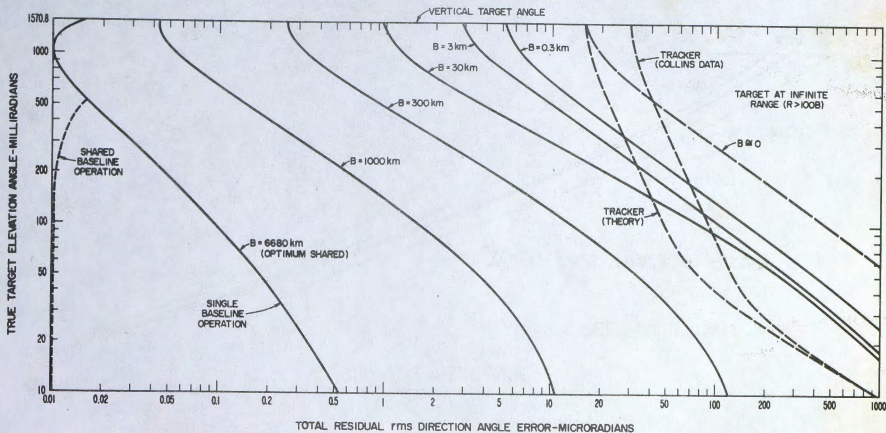
Figure 7. Total systematic and random residual baseline tracking system refraction errors, target at infinite range. Total of systematic and random (angular scintillation) errors of tracking radar also shown, both theoretical (extrapolated zero baseline data) and observed (from Collins Radio Co. data).
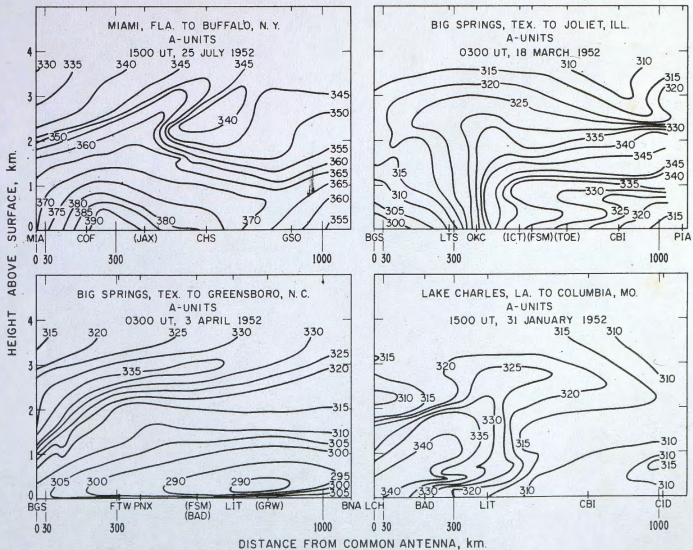
Figure 8. A-unit refractive index structure derived from radiosonde data along four hypothetical baseline paths.
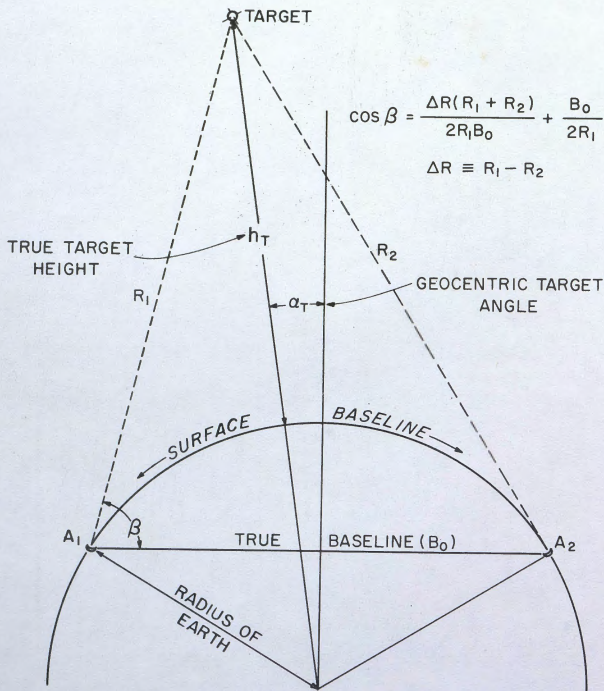
Figure 9. Deep-space baseline tracking system geometry, showing true target position parameters α_t and h_t.

168
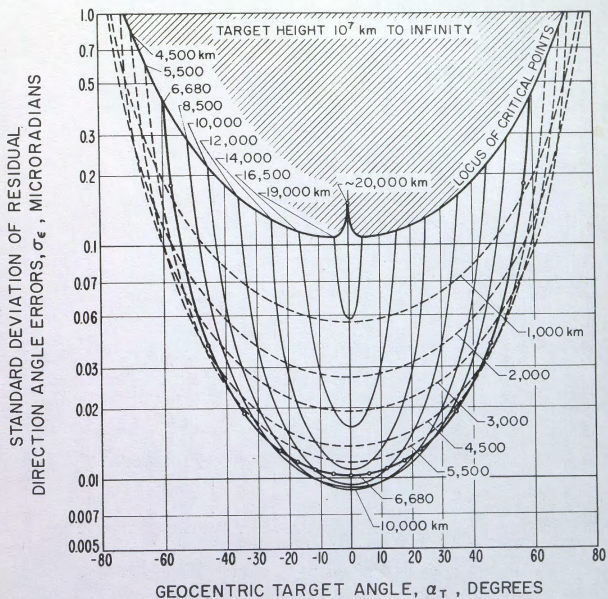
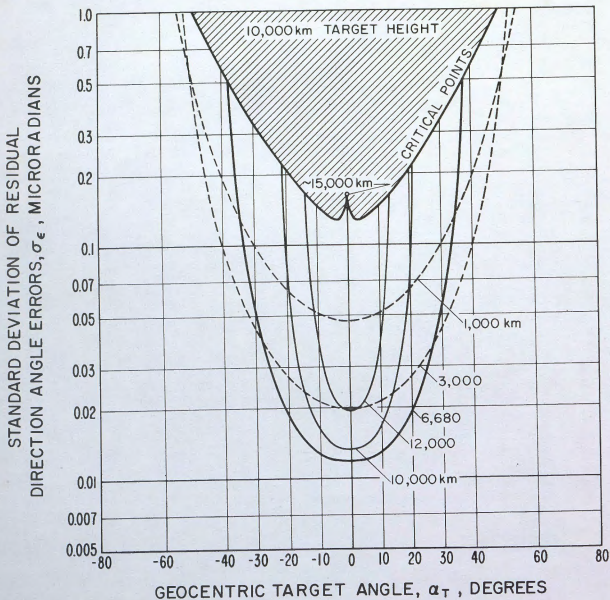Figure 10. Residual direction angle errors of long-baseline tracking systems at very large target ranges.

169

Figure 11. Residual direction angle errors of long-baseline tracking systems at a 10,000 km target height.
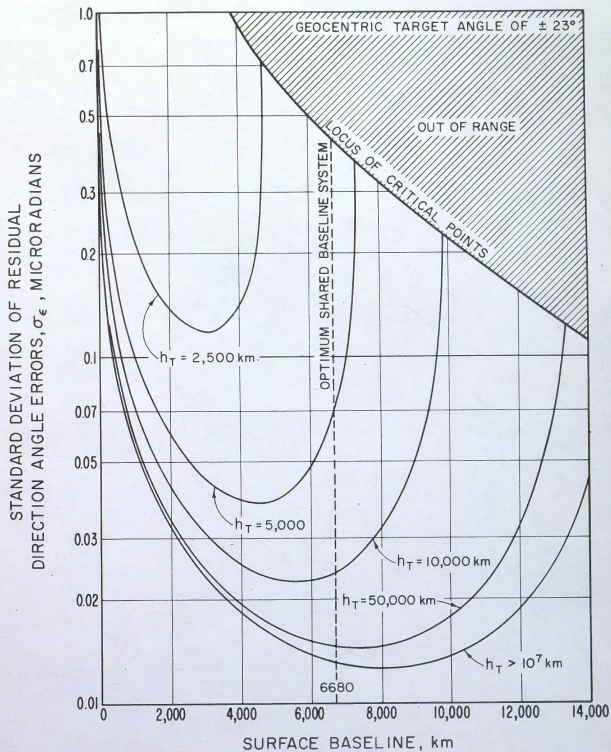
170

Figure 12. Residual direction angle errors of long-baseline tracking systems at a geocentric target angle of ± 23°.
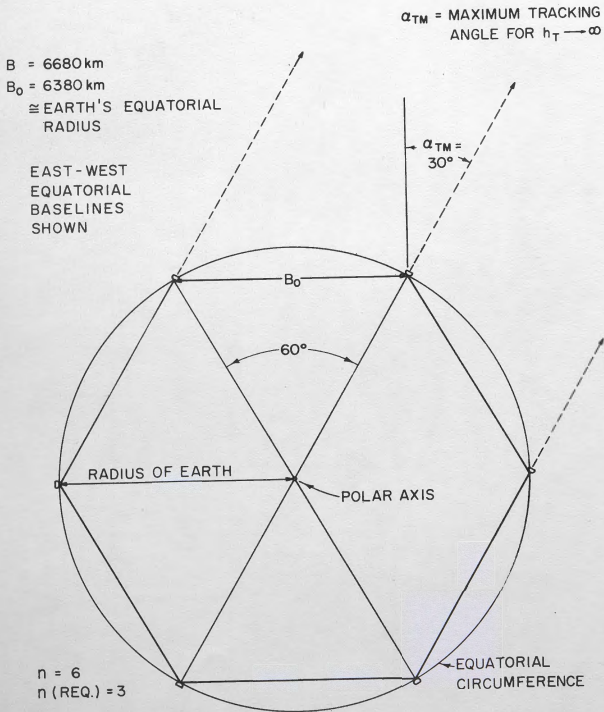
171

Figure 13. Polar plan view of the optimum shared baseline tracking system configuration, showing only the east-west equatorial baselines.
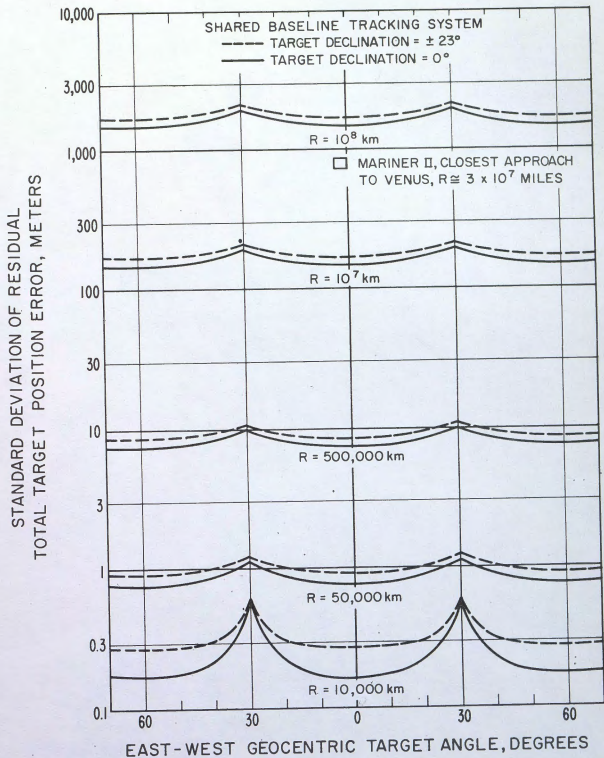
172

Figure 14. Residual rms total target position error for the 6680 km optimum
shared baseline tracking system configuration.

173